Journal of Petroleum
Science and Technology

A Study on the Adsorption and Catalytic Oxidation of Asphaltene onto Nanoparticles

Fatemeh Amin and Ali Reza Solaimany Nazar*

Chemical Engineering Department, University of Isfahan, Isfahan, Iran

ABSTRACT

The use of nanoparticles, including metal oxide surfaces, as asphaltene adsorbents is a potential method of removing and/or upgrading asphaltenes. The adsorption of two asphaltene types, extracted from two types of Iranian crude oil, onto nanoparticles (TiO_2, SiO_2, and Al_2O_3) are assessed and the thermal behavior of the adsorbed asphaltenes is examined under an oxidizing atmosphere through thermogravimetric and differential scanning calorimetry (TG/DSC) analyses. The extracted asphaltenes are characterized through the X-ray diffraction technique, and adsorption isotherms are measured through UV-Vis spectrophotometry of the asphaltene-toluene model solutions. The isotherm data of all the nanoparticles are adequately fitted by the Langmuir model, indicating that asphaltenes form monolayer coverage on solids surface sites. The adsorption capacities of asphaltenes onto the metal oxides follow the order of Al_2O_3> TiO_2> SiO_2. The results indicate that asphaltene with high aromaticity has more adsorption affinity, indicating the effect of the chemical structural of the asphaltenes. The results of asphaltene oxidation tests reveal that the presence of nanoparticles leads to a decrease in oxidation temperature (~100 °C) and activation energy. The effects of nanoparticles on asphaltene oxidation are catalytic.

Keywords: Asphaltene, Nanoparticles, Adsorption Isotherm, Catalytic Oxidation

INTRODUCTION

Crude oil is a very complex mixture containing up to thousands of components. The heaviest fractions of the crude oil are the asphaltenes. Most researchers agree that asphaltenes are a type of polydisperse mixture of molecules containing polynuclear aromatics and aliphatics with small amounts of dispersed heteroatoms like oxygen, sulfur, vanadium, and nitrogen. Asphaltenes are a fraction of the petroleum liquids insoluble in normal alkanes like n-heptane, while soluble in some aromatic solvents like toluene or benzene [1,2]. Asphaltenes are not chemically identifiable compounds, and their composition and structure depend on their source, the method of extraction, and the type of solvents used in extraction [3]. Asphaltene can be adsorbed onto surfaces as colloidal aggregates. Asphaltenes adsorption onto mineral surfaces and reservoir rocks create deposits which affect the oil production rate in a negative sense. The same phenomenon on the upgrading catalyst

***Corresponding author**
Ali Reza Solaimany Nazar
Email: asolaimany@eng.ui.ac.ir
Tel: +98 31 37934027
Fax: +98 31 3793 4031

Article history
Received: December 31, 2015
Received in revised form: June 03, 2016
Accepted: June 11, 2016
Available online: Jun 20, 2017

surface deactivates and contaminates the catalysts [4]. Researchers have applied various surfaces as a means of asphaltene removal. These surfaces include mineral, metallic, and metal oxides surfaces [5-7]. In recent practices, applying nanoparticles of metal oxide, due to their big specific surface area, fast adsorption kinetic, and appropriate dispersion of small particles, is of major concern [2,8-10]. Different nanoparticle types have different asphaltene capacities. The monolayer adsorption of asphaltene onto nanoparticles surface is reported from the toluene model solutions. Researchers have proposed various hypotheses regarding asphaltenes and surfaces bondage. The introduced hypotheses indicate that the asphaltene aromaticity and nitrogen content in its structure is related to asphaltene adsorption [11,12]. In another work [13], contrary to the findings in literature on asphaltene adsorption from model solutions onto nanoparticles, a model of sequential oxidation of adsorbed asphaltenes and multilayer adsorption of asphaltenes from heavy oil types onto prepared in situ and commercial NiO nanoparticles was proposed. It was concluded that NiO nanoparticles did not have catalytic activity towards the oxidation of adsorbed species and limited their function to better expose the adsorbed asphaltenes to the surrounding environment [14]. Researchers continue to assess the thermal oxidation of asphaltene in the presence of nanoparticles. Nassar et al. used different surfaces of Al_2O_3 [15,16], Fe_3O_4, and NiO [12,17] and reported that the nanoparticles can be applied as catalysts to asphaltene oxidation process. The presence of nanoparticles decreases at the oxidation temperature, and the activation energy of the oxidation reactions drops [16,18]. In another study [2,17], it was claimed that the use of nanoparticles for heavy oil upgrading could lead to a reduction in cost. Furthermore, the use of nanoparticles has the potential of being an environment friendly process in heavy oil recovery. The effects of surface acidity and basicity of three categories of metal oxide nanoparticles with acidic (WO_3 and NiO), amphoteric (Fe_2O_3 and ZrO_2), and basic (MgO and $CaCO_3$) surfaces on the thermodynamics of asphaltene adsorption were studied. The results indicate that the asphaltene adsorption capacity of the nanoparticles decreases in the order of NiO >Fe_2O_3 > WO_3 > MgO > $CaCO_3$ > ZrO_2, and the isotherms of the asphaltene adsorption onto the six metal oxides/salts fit the Langmuir model [19].

Nanoparticles application for heavy oil upgrading is a topic of major concern. Thermal cracking performance of an in situ preparation of alumina nanoparticles in heavy oil was assessed and a general shift towards higher API gravity was observed. It was reported that the performance was in uncertainty probably range due to agglomeration at 350 °C, which limits nanoparticle activity [20].

In this work, the adsorption and catalytic oxidation of two types of Iranian crude oil asphaltenes onto nanoparticles are studied and a model is proposed for the asphaltene kinetic decomposition. Herein, the issue in the context of exploring the potential effect of nanoparticles in heavy oil upgrading through the removal or decomposition of asphaltene is addressed; moreover, the adsorption affinity and the catalytic oxidation of asphaltene over nanoparticles are correlated to the asphaltene structural characteristics.

EXPERIMENTAL PROCEDURES

Materials

Herein, three commercially available nanoparticles of SiO_2, Al_2O_3, and TiO_2 are provided from TECNAN (Spain). The reported particle size and specific surfaces area are tabulated in Table 1. The asphaltenes are extracted from two different crude oil types both from south Iran. The SARA analyses of the crude

oil types are tabulated in Table 2. The solvents used in the precipitation and extraction of asphaltene are n-heptane and toluene (analytical grade: Merck, Germany).

Asphaltene Extraction and Model Solution

The residues are extracted from crude oil using atmospheric distillation instrument according to ASTM D86-01. The asphaltenes are extracted from the residues according to ASTM D6560-00. The asphaltenes are dissolved in toluene for the preparation of an 8000 ppm stock solution. The concentration of asphaltene solutions used in the adsorption experiments are within a 100 to 7000 ppm range.

Asphaltene Characterization

Asphaltene characterization is carried out by X-ray diffraction (XRD) analysis. The XRD measurement is made through a Bruker automated diffractometer, applying the CuKα (=1.5406 Å) wavelength. A nickel detector is used to collect the diffraction signals. The diffraction angle (2θ) is scanned from 5° to 45° at a 0.005 (2θ/sec) scan rate with a 2 (sec/step) step size.

Adsorption Experiment

The amount of 0.1 g of nanoparticles is added to the 10 mL model solution of asphaltenes. The samples are shaken in a shaker incubator (NB-205V, N-Biotek instrument Korea, Inc.) at 300 rpm and at 25 °C for about 150 min in order to achieve adsorption equilibrium. The nanoparticles containing asphaltene are centrifuged (Supra 22 K, Hanil instrument Korea, Inc.) for 15 min at 5000 rpm in order to remove the suspended nanoparticles. The separated mixture of asphaltene and toluene is placed in an oven at 50 °C for 20 min in order to have any remained toluene evaporated, and the dried sample is subjected to thermal analysis. The asphaltene concentration in the supernatant is determined by an UV-visible spectrophotometer (V570, Jasco instrument USA, Inc.). A calibration curve of UV-visible absorbance at ~ 800 nm is obtained using standard model solutions with known asphaltene concentrations. The adsorption of asphaltenes onto the nanoparticles is evaluated by measuring the concentrations of the asphaltene in the solution before and after mixing them with nanoparticles. The amount of the adsorbed asphaltenes represented by q_t (mg/m^2) is calculated through the following equation:

$$q_t = \frac{C_0 - C_t}{A \times m} V \quad (1)$$

where, V is the sample volume (L), and m represents the mass of the nanoparticles (g); A is the specific surface area (m^2/g), and C_o stands for the initial concentration of asphaltenes in the solution (mg/L); C_t is the concentration of asphaltenes in the solution at a given time, t, (mg/L).

Thermogravimetric and Differential Scanning Calorimetry (TG/DSC) Analysis of Asphaltene

An amount of 5 mg of asphaltene and the same amount of adsorbed asphaltene onto nanoparticles are heated under air atmosphere (TGA/DSC, L81/1750, Linseis instrument, Inc.). The sample mass is kept low in order to avoid diffusion limitations. The air flow rate is set at 100 cm^3/min. The equipment cell is heated up to 1000 °C at a rate of 10 °C/min in order to get a profile of mass loss and heat changes.

RESULTS AND DISCUSSION

Asphaltene Characterization

The XRD patterns for both samples are shown in Figure 1. The volumes of the characterized parameters are obtained from the XRD measurements of the extracted asphaltene samples (see Table 3). All the terms are determined through the available equations in the related literature [1,21]. The aromaticity (f_a) is the content ratio of aromatic hydrocarbons to all hydrocarbons (aromatic and saturated hydrocarbon). The aromaticity is determined by calculating the areas

of the peaks for the γ and the graphene bands [22]. The aromaticity of asphaltene type 2 is greater than that of type 1; therefore, the asphaltene type 2 is more polar than type 1. It is expected that the interaction type π-π among aromatic rings yield a higher asphaltene precipitation in the asphaltene with more aromaticity. The factor *M* indicates the tendency of aromatics layers aggregation, which has an essential contribution to the asphaltene aggregate formation in a solvent. The d_m, d_γ, and L_c represent the distance among sequential aromatic layers, aliphatic layers, and the average diameter of the aromatic aggregates respectively.

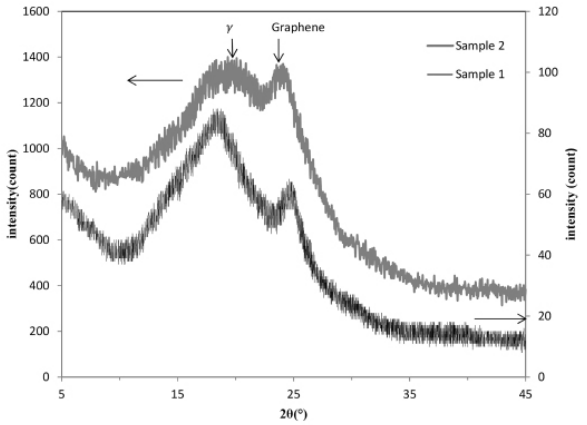

Figure 1: X-ray diffraction patterns of two Iranian crude asphaltenes.

Adsorption Isotherms

The amount of the adsorption of asphaltenes onto nanoparticles is measured at 25 °C by varying the initial concentrations of asphaltene. The adsorption isotherms of asphaltenes onto nanoparticles are shown in Figures 2 and 3. The Langmuir and Freundlich models are adopted to describe the adsorption isotherms through Equations 2 and 3 respectively [23]. The Langmuir isotherm refers to homogeneous adsorption, and the Freundlich isotherm is an empirical expression, which models the multilayer formation of a heterogeneous surface [24].

$$Q_e = Q_m \frac{K_L C_e}{1 + K_L C_e} \quad (2)$$

$$Q_e = K_F C_e^{1/n} \quad (3)$$

The linearized form of Langmuir and Freundlich isotherms are presented through Equations 4 and 5 respectively.

$$\frac{C_e}{Q_e} = \frac{1}{Q_m K_L} + \frac{C_e}{Q_m} \quad (4)$$

$$Log(Q_e) = Log(K_F) + \frac{1}{n} Log(C_e) \quad (5)$$

where, Q_e is the amount of asphaltenes adsorbed onto the nanoparticles (mg/m^2), and K_L is the Langmuir equilibrium adsorption constant related to the affinity of binding sites (L/mg); Q_m stands for the maximum adsorbed amount of asphaltenes per mass of nanoparticles for complete monolayer coverage (mg/m^2), and K_F is the Freundlich constant related to the adsorption capacity ((mg/m^2) (L/mg)$^{1/n}$); *n* is the adsorption intensity factor (dimensionless). The model regressed parameters of the results are listed in Table 4. The values of correlation coefficients (R^2) are used to select the best adsorption isotherm model. The R^2 value is valid as a test of the goodness of fit for one model to multiple data sets. It confirms whether the proposed linear model fits one data set better than another. According to the values of R^2, the Langmuir adsorption isotherm is an appropriate model for predicting the adsorption of asphaltenes onto nanoparticles. The Langmuir-type adsorption isotherms indicate the formation of a monolayer of asphaltenes at the toluene-nanoparticles interface. Ranking the values of Q_m of the selected metal oxides follows in the order of Al_2O_3>TiO_2>SiO_2, and K_L follows the SiO_2>Al_2O_3>TiO_2 order. Similar observations are reported by other researchers for the adsorption of asphaltenes onto different minerals, metals, and metal oxides nanoparticles [5-7, 18]. Dudasova et al. (2008)

reported that these differences can be attributed to the two physical quantities that reflect two different (but linked) phenomena, namely K_L, which contains information on interactions between the adsorbent and adsorbant (asphaltenes and nanoparticles surface) and Q_m, which describes the interactions and the conformation of asphaltenes at the interface [25].

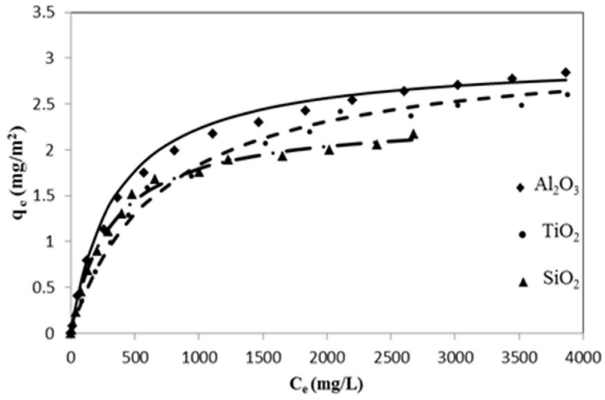

Figure 2: Adsorption isotherm of the first type of asphaltene on different nanoparticles; nanoparticle dose= 10 g/L; agitation speed= 300 rpm; T= 25 °C; the symbols are experimental data, and the solid lines show the Langmuir model.

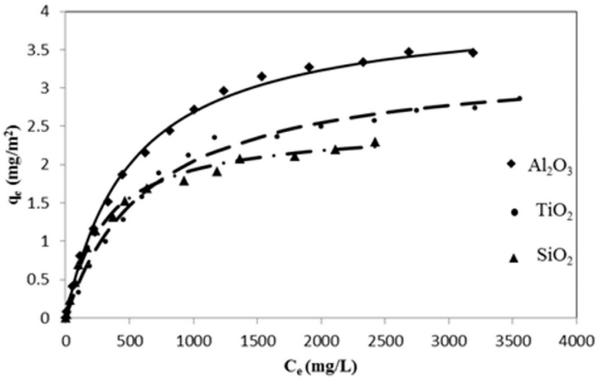

Figure 3: Adsorption isotherm of the second type of asphaltene on different nanoparticles; nanoparticle dose= 10 g/L; agitation speed= 300 rpm; T= 25 °C. The symbols are experimental data, and the solid lines show the Langmuir model.

The adsorption amount of type 2 asphaltene is more than that of type 1, which could be due to higher asphaltene aromaticity in type 2. An increase in asphaltene aromaticity increases the asphaltene polarity; consequently, the polar interactions of asphaltene-asphaltene and asphaltene-nanoparticles cause asphaltene adsorption. Lopez-Linares et al. (2009) concluded that there exists a correlation between asphaltene adsorption and aromaticity [11]. The asphaltene adsorption behavior from asphaltene model solution to a solid interface is related to bulk aggregate characteristics. The asphaltene molecules tendency in aggregate formation, as revealed by M parameter (Table 3), is higher for the asphaltene type 2 than type 1, which suggests more adsorption capacities of the nanoparticles studied here.

Asphaltene Oxidation

The effect of nanoparticle on asphaltene oxidation is assessed by TG and DSC analyses simultaneously. In order to assess the effect of nanoparticles in the asphaltene oxidation process, the asphaltene type with a higher K_L value (type 2) is selected.

Oxidation Temperature Evaluation

The mass variation of the samples as a function of temperature is shown in Figures 4 and 5. The main change in the mass of pure asphaltenes occurs within a temperature range of 400 to 800 °C, while the oxidation of asphaltenes with nanoparticles occurs within a temperature range of 300 to 600 °C. This finding indicates a decrease in the temperature of oxidation in the presence of nanoparticles.

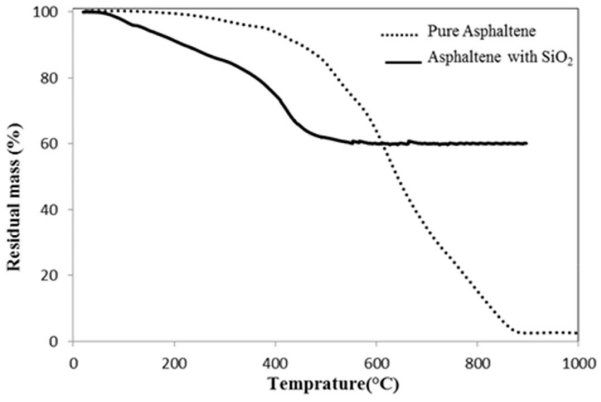

Figure 4: TG curves for the first type of asphaltene with or without SiO_2: plot of residual mass as a function of temperature; heating rate= 10 °C/min; air flow= 100 cm³/min.

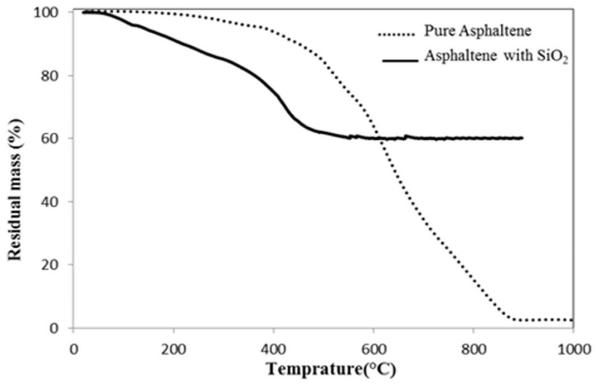

Figure 5: TG curves for the second type of asphaltene with or without nanoparticles; plot of residual mass as a function of temperature; heating rate= 10 °C/min; air flow= 100 cm^3/min.

The results of DSC indicate that the thermal properties of asphaltene-adsorbent are affected by incorporating the nanoparticles in the matrix. As shown in Figures 6 and 7, the exothermic reactions for pure asphaltene occur at temperatures close to 600 °C, whereas the adsorbed asphaltene curves of SiO_2, Al_2O_3, and TiO_2 nanoparticles indicate exothermic peaks at 400, 450, and 500 °C respectively, which indicates a decrease in the oxidation temperature of such compounds with respect to these nanoparticles (Figure 7). By comparing the lower specific surface area of Al_2O_3 and TiO_2 with the higher specific surface area of SiO_2, it becomes clear that the essential sites of the adsorption and catalytic transformation of these nanoparticles are less than those of SiO_2; hence, a lesser catalytic oxidation occurs through these nanoparticles.

The TG curves of asphaltenes with nanoparticles show changes in the samples mass close to zero, and their oxidation is completed in temperatures above 550 °C. A change in the enthalpy of the samples above 550 °C is due to the adsorbent, not the asphaltene.

According to the TG and DSC results, regarding the oxidation of the pure asphaltene and the asphaltene adsorbed onto nanoparticles, it becomes evident that the oxidation reactions mechanism in the presence of nanoparticles leads to major changes in the DSC and TG curves. These changes indicate the nanoparticles catalytic activity. The pure asphaltene oxidation reactions occur homogeneously, while in the presence of nanoparticles it can occur in a heterogeneous manner. These changes in the reaction mechanism lead to the observation of a change in the asphaltene DSC/TG curves with or without nanoparticles.

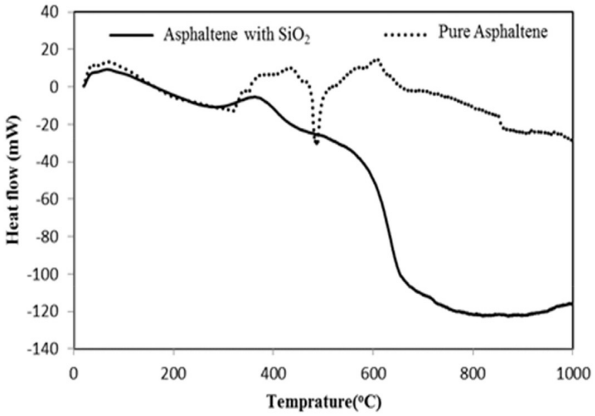

Figure 6: Figure 6: DSC curves for first type of asphaltene with or without SiO_2. Plot of enthalpy change as a function of temperature. Heating rate, 10 °C/min; air flow, 100 cm^3/min.

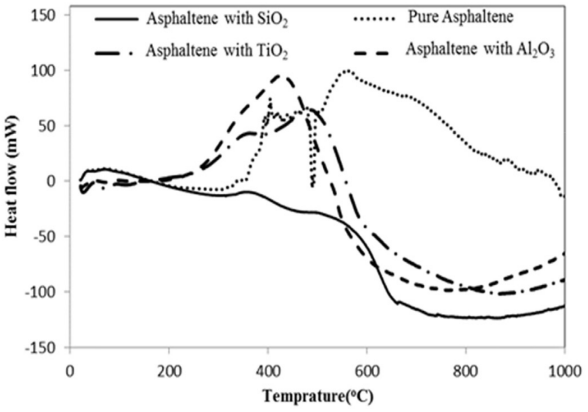

Figure 7: DSC curves for second type of asphaltene with or without nanoparticles. Plot of enthalpy change as a function of temperature. Heating rate, 10 °C/min; air flow, 100 cm^3/min

Estimation of Activation Energy

Activation energy can be calculated through processing the thermogravimetric analytic data. All the methods of activation energy estimation are based on the fraction of conversion (α) and the conversion rate (dα/dt) [26]. The fraction of conversion is defined by:

$$\alpha = \frac{m_0 - m_t}{m_t - m_\infty} \quad (6)$$

where, m_0 is the initial sample mass, and m_t is the sample mass at any given time, t; m_∞ is the final sample mass.

The most commonly used equation in describing the conversion rate in the non-isothermal decomposition kinetics is expressed as the product of independent temperature and reaction mechanism functions:

$$\frac{d\alpha}{dt} = k(T)\, f(\alpha) \quad (7)$$

Arrhenius equation is considered as a temperature function *(K(T))* and $f(\alpha)=(1-\alpha)^n$ describing the mechanism of reaction(s), where, n is the order of reaction. According to the Coats-Redfern method [27], by replacing the above definitions in Equation 7 and then by performing an integration, Equations 8 and 9 are yielded for cases n=1 and n>1 respectively.

$$ln\frac{-\ln(1-\alpha)}{T^2} = \ln\left(\frac{AR}{\beta E_a}\right) - \frac{E_a}{RT} \quad n=1 \quad (8)$$

$$ln\frac{1-(1-\alpha)^n}{(1-\alpha)T^2} = \ln\left(\frac{AR}{\beta E_a}\right) - \frac{E_a}{RT} \quad n>1 \quad (9)$$

where, A is the Arrhenius constant, and T represents the temperature (K); β is the heating rate *(dT/dt),* and R stands for the ideal gas constant (8.314 J/mol.K); E_a is the activation energy.

A plot of the left-hand-side of Equation 8 (assuming *n=1*) versus *1/T* represents a straight line with a slope of E_a/R. The fraction of conversion (α) for the second type of asphaltene with and without nanoparticles as a function of temperature is shown in Figure 8. At any specific temperature, the presence of nanoparticles increases the amount of conversion. The calculated activation energy is tabulated in Table 5. It is inferred from this table that the presence of nanoparticles leads to a decrease in oxidation temperature and the activation energy, indicating the catalytic effect. The catalytic activity of the nanoparticles towards asphaltene oxidation is confirmed by estimating an activation energy lower than the one in the absence of the nanoparticles. The active sites of nanoparticles catalyze the oxidation reaction, thereby lowering the oxidation temperature of the adsorbed asphaltene significantly.

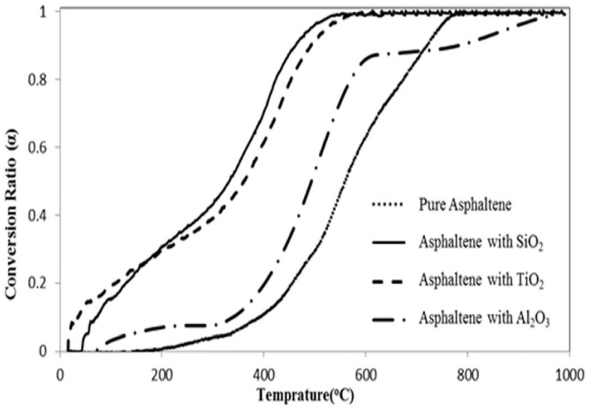

Figure 8: Fraction of conversion (α) for the second type of asphaltene with or without nanoparticles as a function of temperature.

To better understand whether the presence of nanoparticles in the oxidation process could convert the heavy molecules of asphaltene into light weight molecules, more analytical experiments like X-ray photoelectron spectra (XPS) are necessary for further studies.

CONCLUSIONS

The application of TiO_2, Al_2O_3, and SiO_2 nanoparticles in the adsorption and catalytic oxidation processes of asphaltene in asphaltene-toluene model solution is assessed. The adsorption study confirms that the adsorption isotherms of the asphaltene types extracted from two Iranian crude oil types follow

the Langmuir models, so the adsorbed asphaltene on nanoparticles surfaces are monolayer. The Al_2O_3 has the highest adsorption capacities in both of the samples. The aromaticity of the asphaltene type 2 is more than that of asphaltene type 1, indicating a higher polar interaction between asphaltene and nanoparticles with a more adsorption affinity for all nanoparticles. The asphaltene adsorption behavior is correlated to the asphaltene structural characteristics. The comparison of the asphaltene oxidation with or without nanoparticles determines the nanoparticles catalytic effects. The exothermic reactions in the pure asphaltene occur at temperatures close to 600 °C, whereas the asphaltene adsorbed on SiO_2, Al_2O_3, and TiO_2 nanoparticles indicates exothermic peaks at 400, 450, and 500 °C respectively. The estimated activation energies of the asphaltene type 2 oxidation on the nanoparticles indicate an increase in the following order: SiO_2< TiO_2< Al_2O_3. The SiO_2 contributes most to a decrease in the activation energy and the oxidation temperature in comparison with the other nanoparticles used in this study.

REFERENCES

1. Bouhadda Y., Bormann D., Sheu E., Bendedouch D. et al., "Characterization of Algerian Hassi-Messaoud Asphaltene Structure Using Raman Spectrometry and X-ray Diffraction," *Fuel*, **2007**, *86*,1855-1864.
2. Nassar N. N., "Asphaltene Adsorption onto Alumina Nanoparticles: Kinetics and Thermodynamic Studies," *Energy Fuels*, **2010**, *24*, 4116-4122.
3. Groenzin H. and Mullins O. C., "Molecular Size and Structure of Asphaltenes from Various Sources," *Energy Fuels*, **2000**, *14*, 677-684.
4. Syunyaev R. Z., Balabin R. M., Akhatov I. S., and Safieva J. O., "Adsorption of Petroleum Asphaltenes onto Reservoir Rock Sands Studied by Near-Infrared (NIR) Spectroscopy," E*nergy Fuels*, **2009**, *23*, 1230-1236.
5. Alboudwarej H., Pole D., Svrcek W. Y., and Yarranton H. W., "Adsorption of Asphaltenes on Metal," *Ind. Eng. Chem. Res*., **2005**, *44*, 5585-5592.
6. Marczewski A. W. and Szymula M., "Adsorption of Asphaltenes from Toluene on Mineral Surface," *Colloid Surf. A. Physicochem. Eng. Asp*., **2002**, *208,* 259-266.
7. Rudrake A., Karan K., and Horton J. H., "A Combined QCM and XPS Investigation of Asphaltene Adsorption on Metal Surfaces," *J. Colloid Interface Sci*., **2009**, *332*, 22-31.
8. Franco C., Patino E., Benjumea P., Ruiz M. A. et al., "Kinetic and Thermodynamic Equilibrium of Asphaltene Sorption onto Nanoparticles of Nickel Oxide Supported on Nanoparticulated Alumina," *Fuel*, **2013**, *105*, 408-414.
9. Xinhu T. and Dongyang L., "Evaluation of Asphaltene Degradation on Highly Ordered TiO_2 Nanotubular Arrays via Variations in Wettability," *Langmuir*, **2011**, *27*, 1218-1223.
10. Mohammadi M., Akbari M., Fakhroueian Z., Bahramian A. et al., "Inhibition of Asphaltene Precipitation by TiO_2, SiO_2, and ZrO_2 Nanofluids," *Energy Fuels*, **2011**, *25*, 3150-3156.
11. Lopez-Linares F., Carbognani L., Sosa-Stull C., Almao P. P. et al., "Adsorption of Virgin and Visbroken Residue Asphaltenes over Solid Surfaces. 1. Kaolin, Smectite Clay Minerals, and Athabasca Siltstone," *Energy Fuels*, **2009**, *23*, 1901-1908.
12. Nassar N. N., Hassan A., and Almao P. P., "Thermogravimetric Studies on Catalytic Effect of Metal Oxide Nanoparticles on Asphaltene Pyrolysis under Inert Conditions," *J. Therm. Anal. Calorim*., **2012**, *110*, 1327-1332.
13. Tarboush B. J. A. and Hossein M. M., "Adsorption of Asphaltenes from Heavy Oil onto In Situ Prepared NiO Nanoparticles," *J. Colloid Interface Sci*., **2012**, *378*, 64-69.
14. Tarboush B. J. A. and Hossein M. M., "Oxidation of Asphaltenes Adsorbed onto NiO Nanoparticles," *Appl. Catal. A*., **2012**, *445-446*, 166–171.
15. Nassar N. N., Hassan A., and Almao P. P., "Effect of Surface Acidity and Basicity of Alumina on Asphaltene Adsorption and Oxidation," *J. Colloid Interface Sci*., **2011**, *360*, 233-238.
16. Nassar N. N., Hassan A., and Almao P. P., "Effect of Particle Size on Asphaltene Adsorption and Catalytic Oxidation onto Alumina Nanoparticle," *Energy Fuels*, **2011**, *25*, 3961-3965.
17. Nassar N. N., Hassan A., and Almao P. P.,

"Comparative of Adsorbed Asphaltene onto Transition Metal Oxide Nanoparticle," *Colloid Surf.*, **2011**, *384*, 145-149.
18. Nassar N. N., Hassan A., and Almao P. P., "Metal Oxide Nanoparticles for Asphaltene Adsorption and Oxidation," *Energy Fuels*, **2011**, *25*, 1017-1023.
19. Hosseinpour N., Khodadadi A. A., Bahramian A., and Mortazavi Y., "Asphaltene Adsorption onto Acidic/Basic Metal Oxide Nanoparticles Toward in Situ Upgrading of Reservoir Oils by Nanotechnology," *Langmuir*, **2013**, *29*, 14135−14146.
20. Husein M. M. and Alkhaldi S. J., "In Situ Preparation of Alumina Nanoparticles in Heavy Oil and Their Thermal Cracking Performance," *Energy Fuels*, **2014**, *28*, 6563–6569.
21. Shirokoff J. W., Siddiqui M. N., and Ali M. F., "Characterization of the Structure of Saudi Crude Asphaltenes by X-ray Diffraction," *Energy Fuels*, **1997**, *11*, 561-565.
22. Solaimany Nazar A. R. and Bayandory L., "Investigation of Asphaltene Stability in the Iranian Crude Oils," *Iran. J. Chem. Eng*., **2005**, *5*, 3-12.
23. Foo K. Y. and Hameed B. H., "Insights into the Modeling of Adsorption Isotherm Systems," *Chem. Eng. J*., **2010**, *156*, 2-10.
24. Natarajan A., Kuznicki N., Harbottle D., Masliyah J. et al., "Understanding Mechanisms of Asphaltene Adsorption from Organic Solvent on Mica," *Langmuir*, **2014**, *30*, 9370-9377.
25. Dudasova D., Simon S., Hemmingsen P. V., and Sjoblom J., "Study of Asphaltenes Adsorption onto Different Minerals and Clays: Part 1. Experimental Adsorption with UV Depletion Detection," *Colloid Surf*., **2008**, *317*, 1-9.
26. Nunez L., Fraga F., Nunez M. R., and Villanueva M., "Thermogravimetric Study of the Decomposition Process of the System BADGE," *Polymer*, **2000**, *41*, 4635-4641.
27. Coats A. W. and Redfern J. P., "Kinetic Parameters from Thermogravimetric Data," *Nature*, **1964**, *201*, 68-69.